Supplemental Data:

GEF-H1 regulates cell migration via localized activation of RhoA at the leading edge

Perihan Nalbant, Yuan-Chen Chang, Jörg Birkenfeld, Zee-Fen Chang, and Gary M. Bokoch

Figure S1: Transfection efficiency using siRNA and depletion of GEF-H1 in individual Hela cells

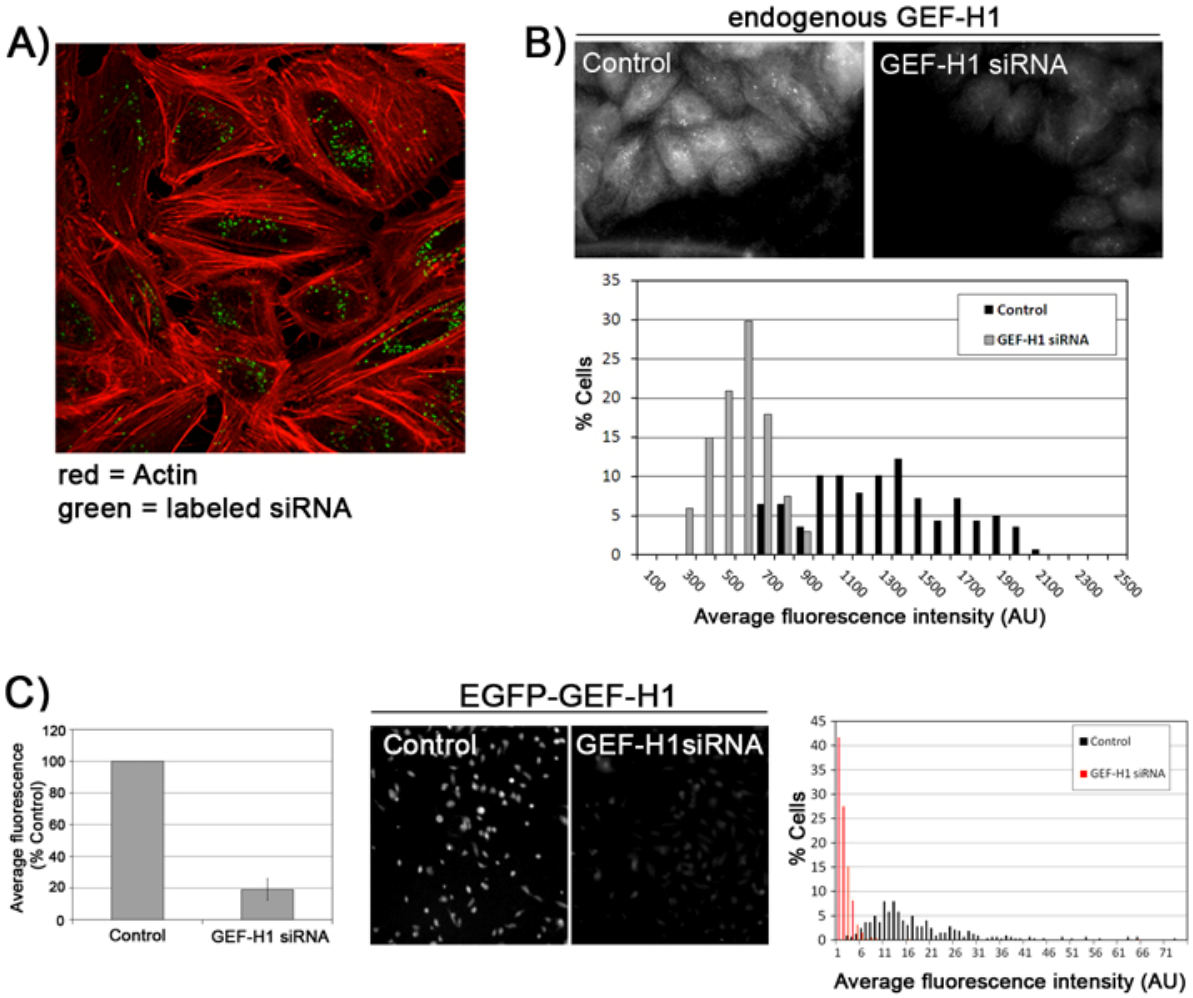

Figure S1: A) Transfection efficiency of siRNA. Hela cells were transfected with Alexa-488 labeled siRNA (Qiagen, Germany) and fixed after 24 hrs using 4% formaldehyde. Cells were then stained with rhodamine-labeled phalloidin to visualize the actin cytoskeleton. Representative image of n =2 independent experiments. In both experiments we measured >95% transfection efficiency (20 randomly chosen fields were examined). B) Endogenous GEF-H1 protein levels in individual cells. Hela cells were transfected with siRNA as described in the Material and Methods. Wound healing cells were fixed and stained using the affinity purified antibody specific for GEF-H1 (Zenke et al., 2004). Images were acquired using same exposure times. After background subtraction, average cytosolic

intensity of GEF-H1 antibody staining was measured using the region tool and standard ImageJ measurement plug-ins (http://rsb.info.gov/ij/). Based on the antibody staining, GEF-H1 siRNA treated cells had on average 56.7% (+/- 3.0) less staining as compared to control cells (n = 2 independent experiments with 184 control and 111 GEF-H1 siRNA treated cells). This result is likely to be an underestimation due to slight unspecific reactivity of the antibody, as our Western blot analyses consistently showed knock-down efficiency > 80 % (see Figure 1A, main manuscript). Lower panel: Based on individual cell analysis, 72 % of the cells had lower average intensity levels than the minimal amount detected in control cells. C) To further characterize the knock-down of GEF-H1 in individual cells we used exogenous expression of EGFP-tagged GEF-H1 (1 μg) after co-transfection with control and GEF-H1 targeting siRNA (20 μM), respectively. 48 hrs post-transfection, cells were fixed with 4% formaldehyde and EGFP-fluorescence of individual cells was quantified. Left: On average, the EGFP signal was strongly decreased in cells co-transfected with GEF-H1 siRNA (81% +/- 6.7%). Results are +/- SD of 2 individual experiments with total number of 959 (control) and 1113 (GEF-H1 siRNA treated) cells. Middle section: Representative images of EGFP-GEF-H1. Images of randomly chosen regions were acquired and processed using same settings for both conditions. Control image shows significantly higher EGFP-signals as compared to the image with cells transfected with GEF-H1-specific siRNA. Right panel: Intensities of individual cells are plotted. Again, the majority of the GEF-H1 siRNA-treated cells had less EGFP signal than the lowest detected amounts in control cells .

Figure S2: Cell viability in siRNA transfected cells

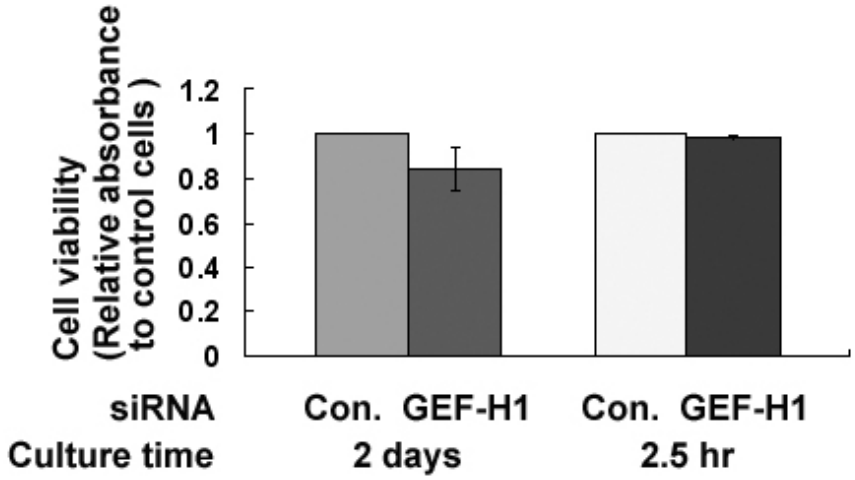

Figure S2: The effect of GEF-H1 knockdown on cell viability was analyzed using MTT assay. siRNA-treated cells were seeded in triplicate at a concentration of either 8×10^4 cells/well for 46 hrs or 3.5×10^5 cells/well for 30 mins in 12-well fibronectin-coated plates (Corning). After the cells had adhered, MTT (3-(4,5-dimethylthiazol-2-yl)-2,5-diphenyltetrazolium bromide) was added to the cells (0.2 mg/ml) at 37 °C for an additional 2 hrs., The cells were then washed with PBS, followed by addition of DMSO (300 μM) for 20 min. Aliquots (100 μl) of the final solutions were transferred into 96-well plates in duplicate and absorbance recorded at 560 nm. Results were analyzed with the Soft max pro4 software and are presented as relative absorbance of the average control values from two independent transfection experiments.

Figure S3: Elevated RhoA activity is associated with highly coordinated ruffling in protrusions

In control Hela cells, we have noticed that RhoA activity was in some instances different in morphologically similar protrusions. Using DIC imaging in parallel to the FRET assay, we were able to investigate the dynamic behavior of the cell edges during the FRET study. In some instances ruffling was assessed using CFP-time-lapse movies as well. Movies were acquired for 4-6 min. Kymograph analysis of 32 control cell protrusions (14 cells) revealed strong correlation between persistent RhoA activity in the leading edge and persistent ruffling within the same region. Of the 32 analyzed protrusions, 24 showed ruffling during the entire time-lapse analysis. RhoA was persistently active in the leading edge of 19 protrusions (79%). Interestingly, activity decreased significantly over time when ruffling slowed down or diminished entirely (4 of 24 ruffling protrusions; 16.7 %). Only in one case could we not detect any significantly elevated RhoA activity in the leading edge despite membrane ruffling.

We also assessed if RhoA activity was associated with protrusiveness of the leading edge of individual cell protrusions. Indeed, leading edge activity of RhoA was persistently eleveated in growing or stable protrusions (23 of 32 analyzed protrusions). Importantly, in each of these cases protrusions were ruffling throughout the time-lapse period. In contrast, shrinkage of extensions was often accompanied by diminished RhoA activity (in 5 of 6 shrinking protrusions).

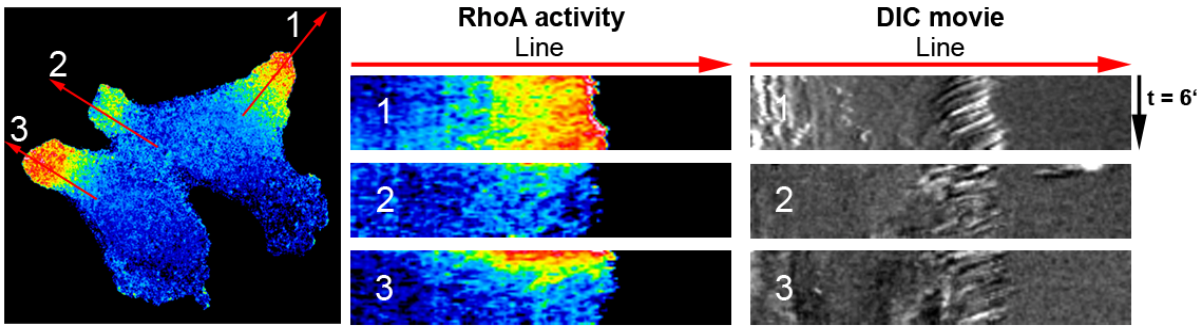

Figure S3: RhoA is activated persistently in protrusions with regular ruffling. Kymograph analysis of FRET movies in combination with DIC time-lapse depict that RhoA is highly activated in protrusions with regular ruffling. Time-lapse movies were acquired for 6 min duration.

Figure S4: Number of ruffling cells is increased upon GEF-H1 depletion

We noticed that cells depleted of GEF-H1 displayed higher tendency to develop ruffles, albeit with significant aberrant dynamics (Figure 3, main manuscript). The number of cells displaying ruffles in control and siRNA transfected cells was scored to quantify this effect.

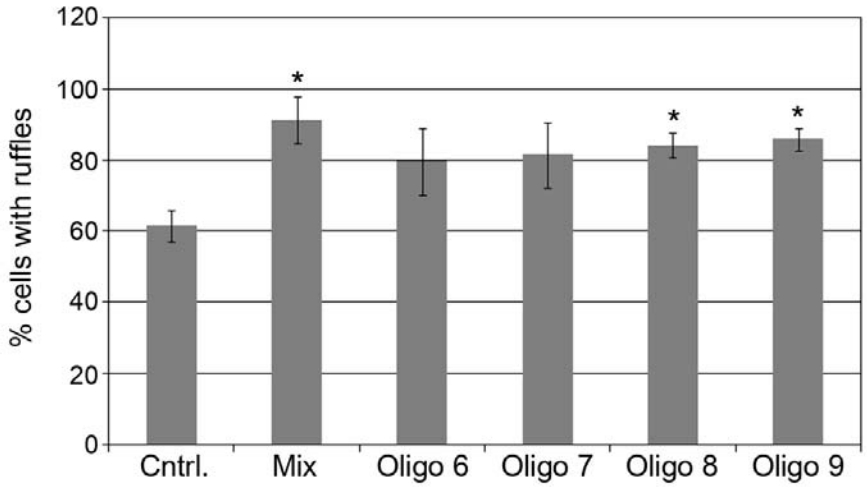

Figure S4: Increased number of ruffling cells due to GEF-H1 depletion. Phase contrast movies with single cells were analyzed. To rule out off-target effects of the GEF-H1 siRNA mix, individual oligonucleotides were also used to deplete GEF-H1 and quantify the number of ruffling cells, in addition to observing leading edge behavior. Results are +/- SD of n = 2 experiments with: control = 178 cells, GEF-H1 siRNA-mix of 4 oligos = 98 cells, oligo 6 = 135 cells, oligo 7 = 228 cells, oligo 8 =203 cells, oligo 9 = 204 cells. P-value < 0.05 = *. *Knock-down of GEF-H1 by each individual oligo was confirmed using immunoblot analysis. The knock-down efficiency was comparable for each condition (see also Birkenfeld et al., 2007).*

Figure S5: Actin density within the leading edge is decreased upon GEF-H1 depletion

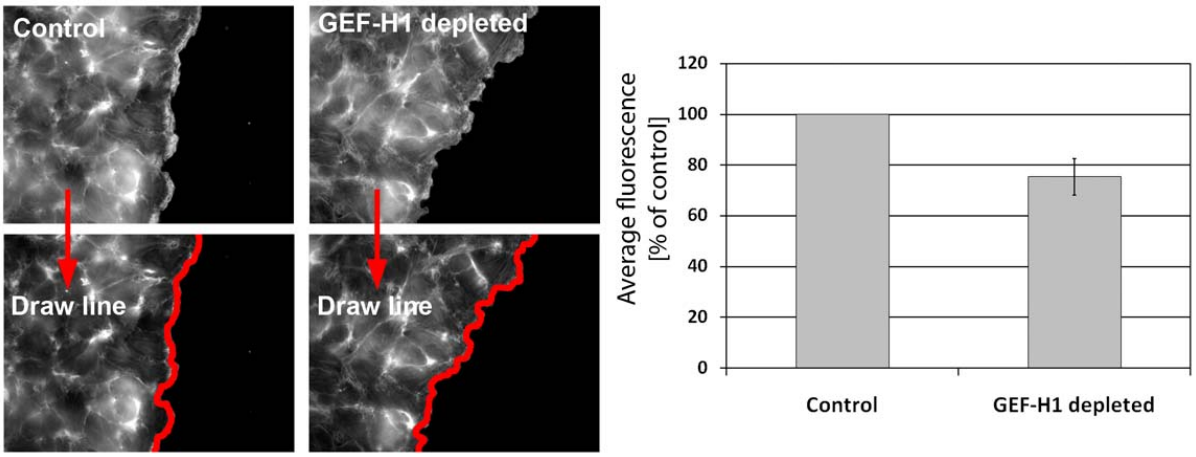

Figure S5: Quantification of actin density in the leading edge of migrating cells. Transfection of siRNA and wound healing experiments were performed as described in the Materials and Methods. Wound healing images were acquired of randomly chosen regions. Each image captured in the experiment was analyzed as follows. Bulk analyses of images were performed using the freehand line tool provided by ImageJ software. Average actin amount within the drawn leading edge region was measured for n = 2 independent experiments (Experiment 1: 52 control, 51 GEF-H1-siRNA images; Experiment 2: 12

control, 13 GEF-siRNA images). For both experiments, statistical significance of the difference was assessed using t-test analysis (Experiment 1: P-value = 0.0000038; Experiment 2: P-value = 0.025).

Figure S6: GEF-H1 is localized to actin rich ruffles – Confocal

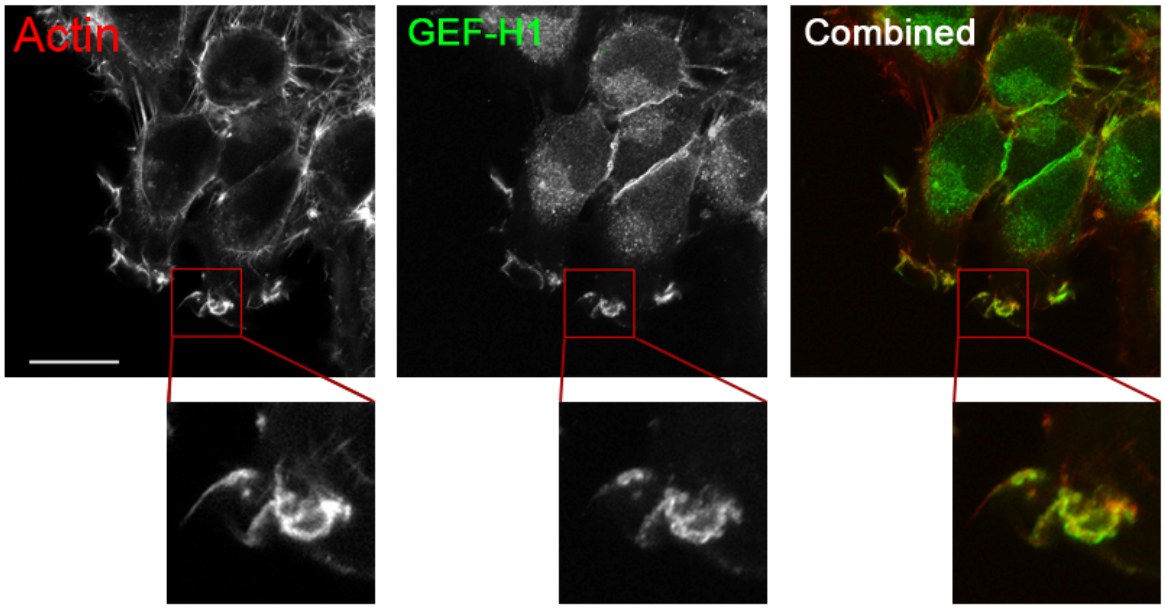

Figure S6: HeLa cells were grown in monolayer and in vitro scratches were generated as described in the Materials and Methods. At 2 hrs post-wound, cells were fixed using formaldehyde and stained for endogenous GEF-H1 with a polyclonal anti-GEF-H1 antibody previously described (Zenke et al., 2004). The actin cytoskeleton was stained with phalloidin labelled with Alexa-568 dye (Invitrogen, Molecular Probes, Carlsbad, CA, USA). Confocal images were obtained on a Bio-Rad MRC2100 Rainbow Radiance system attached to a Nikon TE2000-U using a 60x/1.4 oil objective. Images were processed using the image analysis software ImageJ (http://rsb.info.gov/ij/). Scale bar = 20 μm.

Figure S7: Polarization of MTOC not altered in GEF-H1-depleted cells.

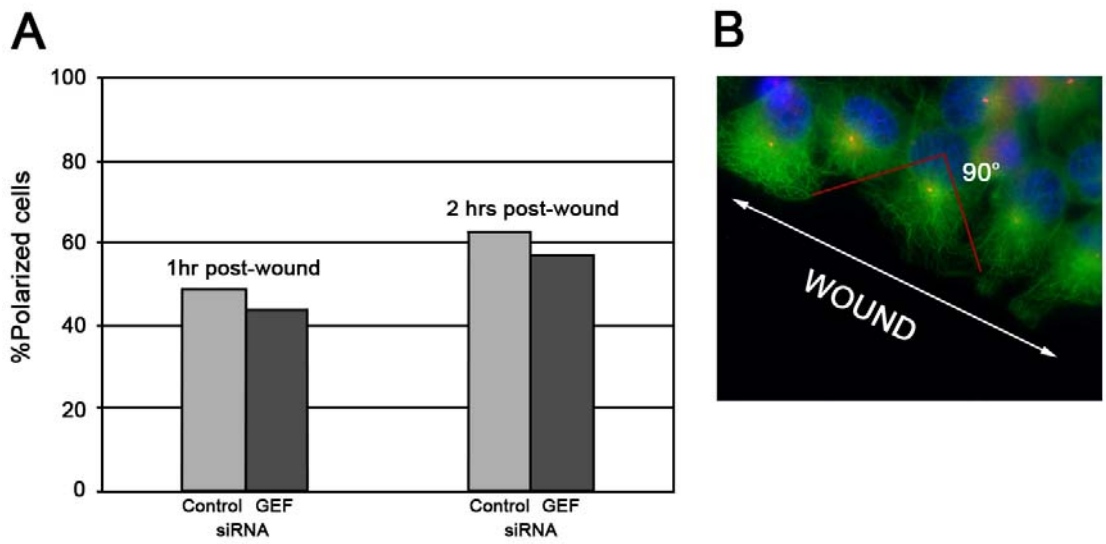

Figure S7: HeLa cells were grown to confluency and in vitro scratches were generated as described in Materials and Methods. Cells were fixed at the indicated time-points using ice-cold methanol and stained for the centrosome protein pericentrin as a marker for the microtubule organizing center (MTOC) (polyclonal antibody, COVANCE, CA, USA) and for α -Tubulin (monoclonal anti-α-Tubulin, clone B-5-1-2, Sigma-Aldrich). Images were acquired on a Nikon TE2000-U using a 20x objective. To assess the polarization of the cells after scratching, the localization of the MTOC was evaluated with respect to the leading edge and the nucleus. Cells were counted as polarized when the MTOC was localized between nucleus and leading edge as depicted in B. Control: 1 hr = 169 cells (15 regions), 2 hrs = 211 cells (14 regions); GEF-H1 depleted: 197 cells (12 regions), 2 hrs = 118 cells (14 regions) were counted.

Figure S8: Quantification of EB1-decorated microtubule tips in the leading edge – protocol

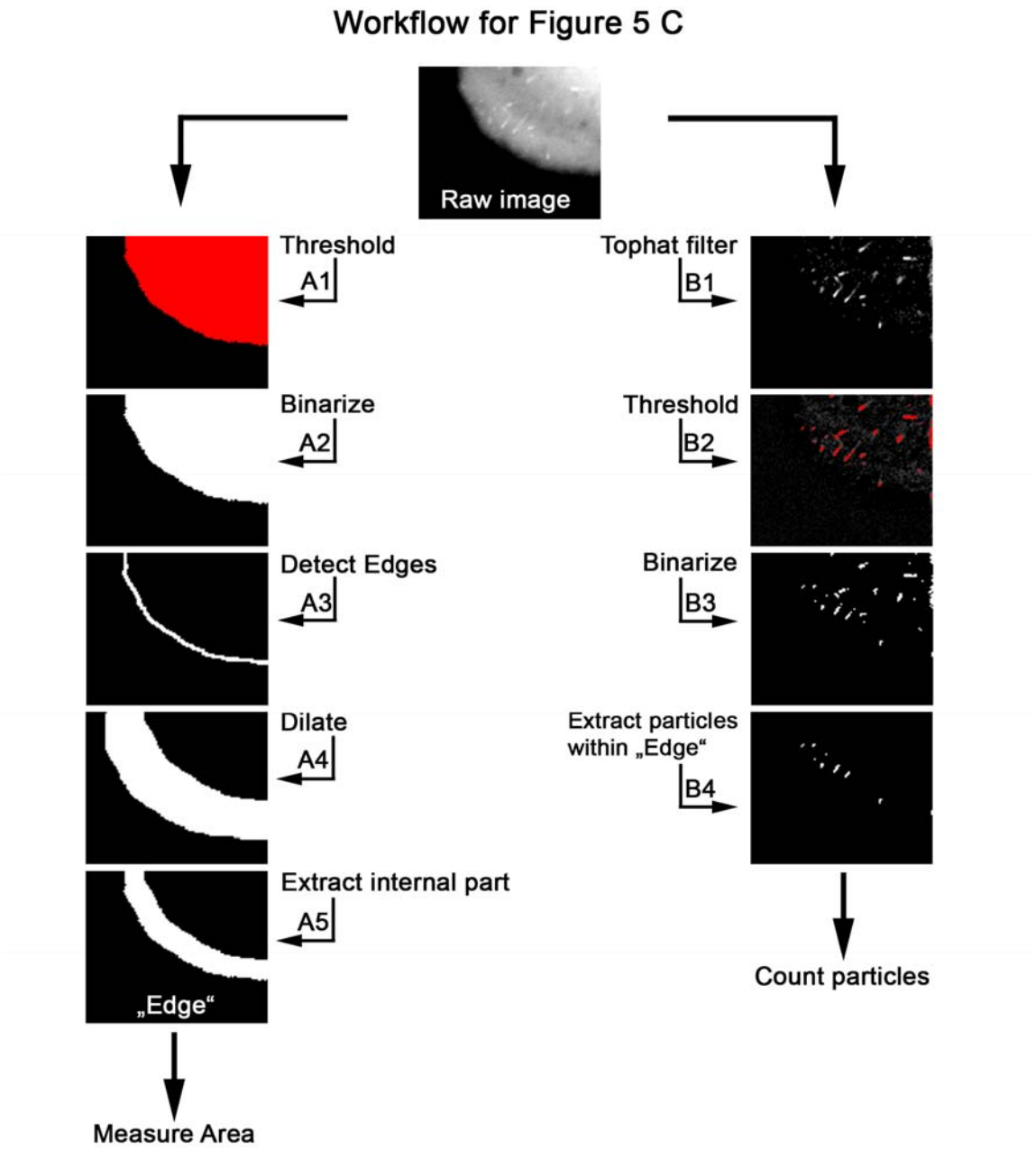

Figure S8: ***Workflow for quantification of microtubule (MT) plus ends in the cell front (used in Figure 5C – main manuscript).*** *EGFP-EB-1 expressing HeLa cells were imaged on a NIKON TE2000-U using a 60x/1.4 oil objective. Time-lapse images were processed using various plugins provided in the ImageJ software (http://rsb.info.gov/ij/). In brief, two lines of image processing were established to measure the number of MT tips approaching the leading edge region during the time-lapse. Binary images (white = value 1, black = value 0) were generated throughout following the indicated operations in order to define specific regions of interest for subsequent processing steps. (**A**) Images were thresholded to obtain a binary mask of the cell area (A1 and A2). The cell edge was detected by the "Find Edges" tool (A3). This line was dilated 10 times to generate a broad band by using the "Dilate" tool (in Process – Binary – Dilate) (A4). As the dilation is applied in both directions from the line, the intracellular part of the broad band was extracted by processing the image A4 with the previously obtained A2 using the "AND" Tool (in Process – Math – AND). As this tool extracts only the areas which are present in both processed images (A2 and A4), the resulting*

*figure represents only the intracellular area (A5). The binary image A5 contains the designated leading edge region in which all pixel values are 1 (in white). By use of additional image based operations it can be processed with other images for the purpose of conducting measurements such as the number of MT-tips detected within this area. (**B**)The second part of the analysis was performed in order to generate a binary image in which the growing MT tips are present as dots with the pixel value 1. First, the EGFP-EB1 dots in the raw image were enhanced using the "Top-Hat" filter plug-in (B1). These images were thresholded so binary images depicting single dots could be generated (B2 and B3). The "AND" tool was applied to the images (A5) and (B3). The resulting image represented the EGFP-EB1 decorated microtubule tips solely within the confined leading edge region (B4). Finally, the number of EGFP-EB-1 dots was counted by using the "Analyze Particles" tool (in Analyze – Analyze Particles), and the value was normalized for the measured area of the leading edge. The settings for the Analyze Particles tool were as follows: Size = 0 – infinity, Circularity = 0.00 – 1.00. Average of the entire time-lapse stack was calculated for each cell.*

Figure S9: Microtubule density is increased in the leading edge of GEF-H1 depleted cells

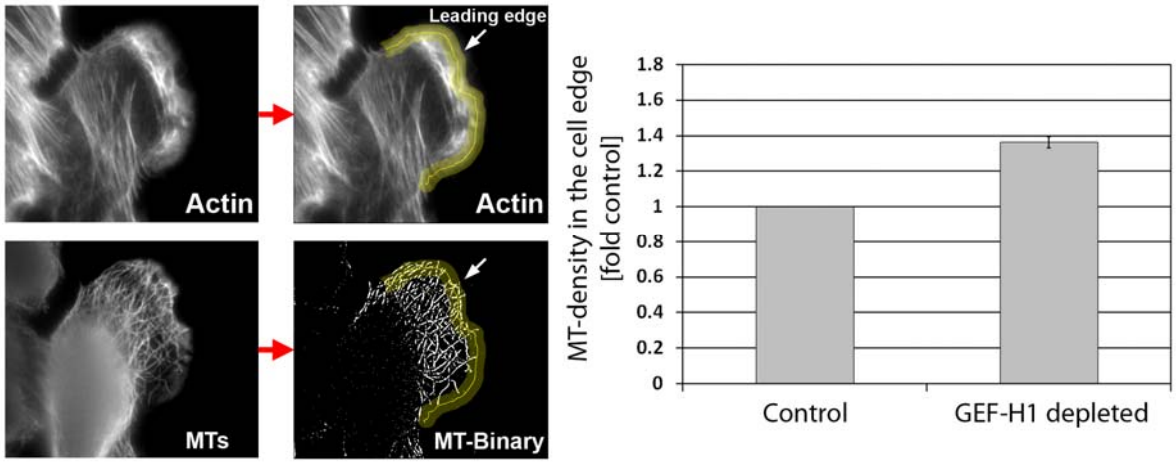

Figure S9: Quantification of microtubule (MT) density in the leading edge. Wound healing experiments were performed as described in the Material and Methods. Microtubules together with actin were visualized using anti-a-tubulin antibody in combination with rhodamine labeled phalloidin. Images were processed using ImagJ software in order to quantitatively measure density of MT within the leading edge. Images of the MT cytoskeleton were subjected to a tophat filter, followed by thresholding in order to generate a binary image (value 1 for MT or 0 for no MT). Using the freehand line tool, a 3 um wide region was generated based on the actin image as template and applied to the binary image. Density of MTs in the leading edge region was measured using the built-in measure tool (ImageJ). As in the time-lapse studies tracking EB-1 decorated MT tips, measurement in fixed cells showed increase of MTs in the immediate leading edge region when GEF-H1 was depleted. Results are +/- SD from 2 independent experiments (Experiment 1: 62 control, 60 GEF-H1 depleted cells; Experiment 2: 37 control, 46 GEF-H1 depleted cells). In each experiment, statistical analysis revealed significant difference between the two conditions (Experiment 1: p-value = 0.001; Experiment 2: p-value = 0.000082).

Figure S10: PAK phosphorylation is not altered in GEF-H1 depleted HeLa cells

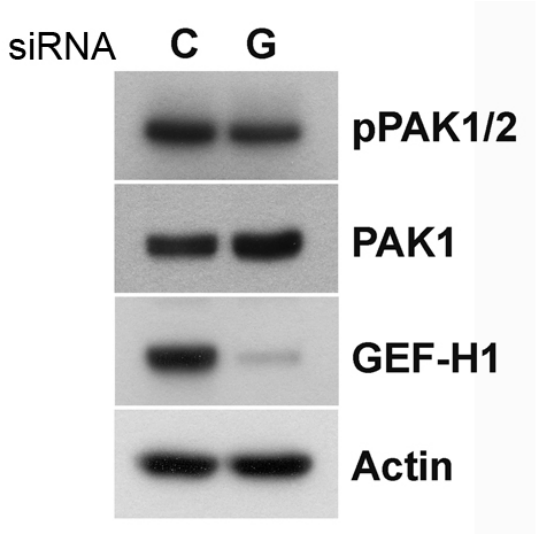

Figure S10: Cells were lysed as described in Materials and Methods. Cell lysates were separated by SDS-PAGE and immunoblotted with anti pPAK1/2 antibody. No significant difference in overall pPAK1/2 could be detected between control and GEF-H1-depleted cells. There was also no difference in pPAK1/2 distribution detected at the leading edge by immunofluorescence microscopy (not shown).

Figure S11: Cell-cell contacts are not altered in GEF-H1-depleted cells

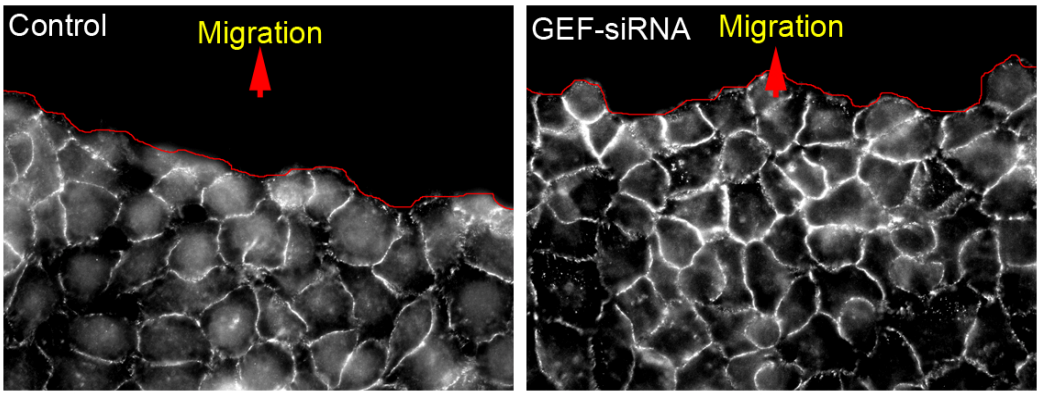

Figure S11: HeLa cells were plated on glass coverslips, transfected with control or GEF-H1 siRNA and grown until confluency. The cells were methanol-fixed 2 hrs post-scratch formation and stained using anti-N-cadherin antibody (13A9, 1:500 dilution, Millipore). The wound-edge is depicted in red. Cell-cell contacts were in general of similar shape and thickness. Direction of migration is indicated by the red arrows.

Supplemental movies (representative images):

Movie S1: Migrating Hela cells.

Movie S1A: Randomly migrating HeLa cells

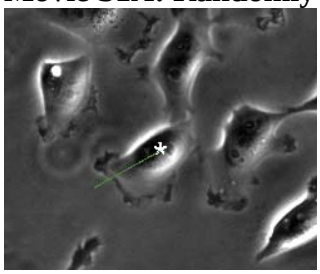

HeLa cells were plated on FN-coated coverslip sparsely over night, and then recorded by MetaMorph software at 30 second intervals for 1 hr. Cell migration followed the direction of ruffling. The green line shows the track of migrating cells during the time-lapse recording.

Movie S1B: Directional migration of HeLa cells in a wound

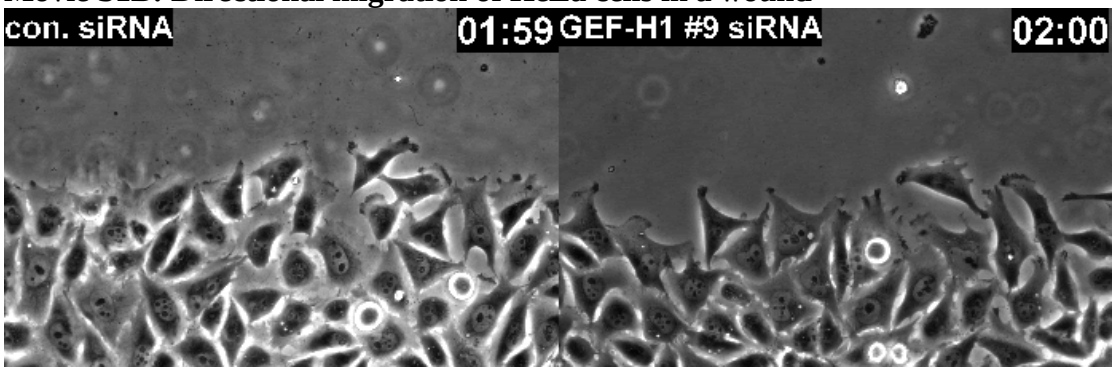

Confluent control and GEF-H1-specific #9 siRNA treated cells were scratched and then recorded by Metamorph software at 1 minute intervals for 2 hrs to observe directional motility. Left panel, control siRNA; Right panel, GEF-H1 #9 siRNA.

Movie S2: Leading edge dynamics

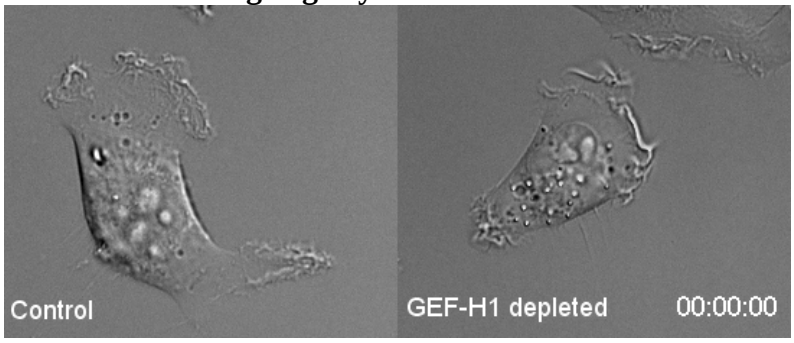

Movie S2: Leading edge dynamics in control and GEF-H1 depleted cells. Differential interference contrast (DIC) images were acquired with a 60x/1.4 NA oil objective in 5 sec intervals.

Movie S3A: RhoA activation dynamics in control HeLa cells

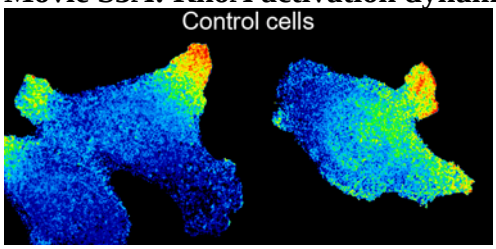

Movie S3B: RhoA activation dynamics in GEF-H1 depleted HeLa cells

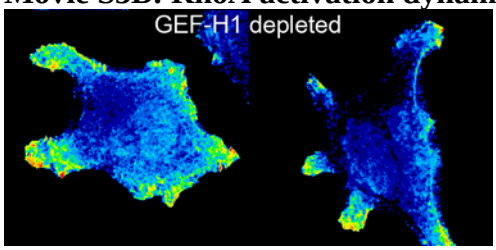

Movies S3 A and B: HeLa cells stably expressing the RhoA activation probe were observed during random migration. Time-frame = 10 sec

Movie S4: Actin dynamics in the leading edge

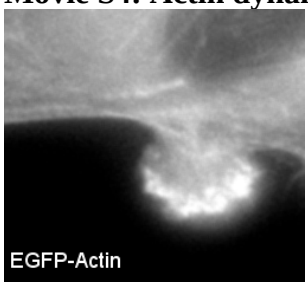

Movie S4: Control HeLa cells were transfected with EGFP-Actin. Frame rate: 5 sec

Movie S5: EGFP-EB-1 time-lapse analysis

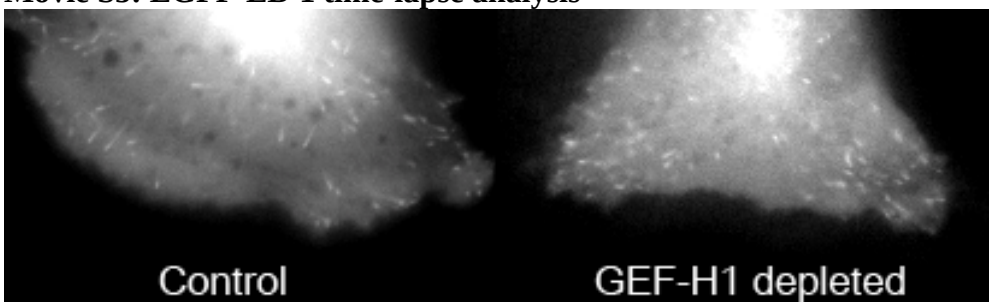

Movie S5: Time-lapse imaging of EGFP-tagged EB-1 in control and GEF-H1 cells. Cells were transfected with control and GEF-H1 siRNA, respectively. At 48 hrs post-siRNA, EGFP-EB-1 plasmid was transfected. Imaging was conducted at 72 hrs after siRNA treatment. Frame rate: 5 sec

Movie S6: Quantification of MT tips in the leading edge – descriptive movie

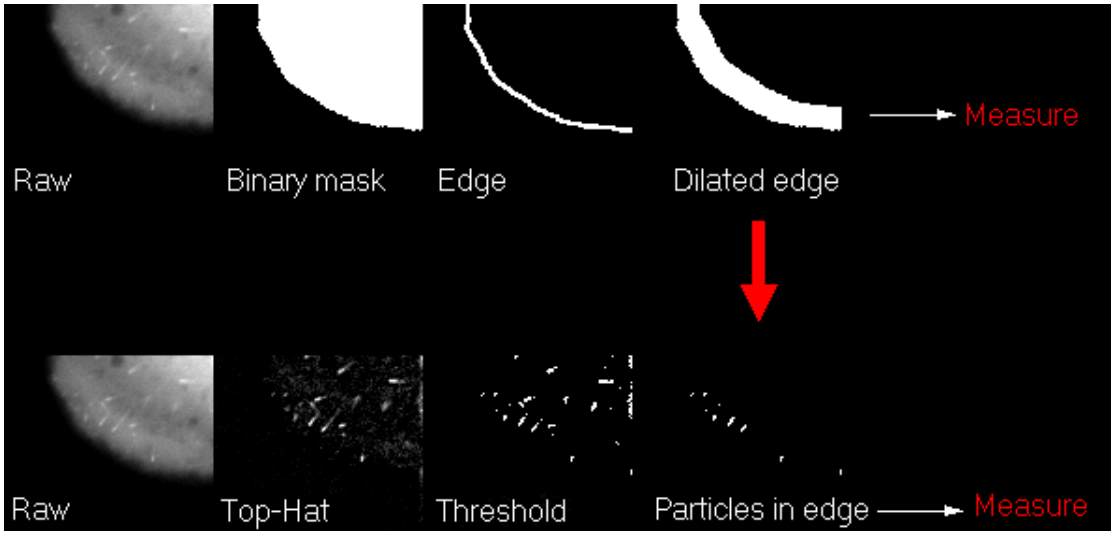

Movie S6: Quantification of EGFP-EB-1 decorated MT tips in the leading edge. For detailed protocol, see Supplemental Materials.

Movie S7: Focal adhesion dynamics

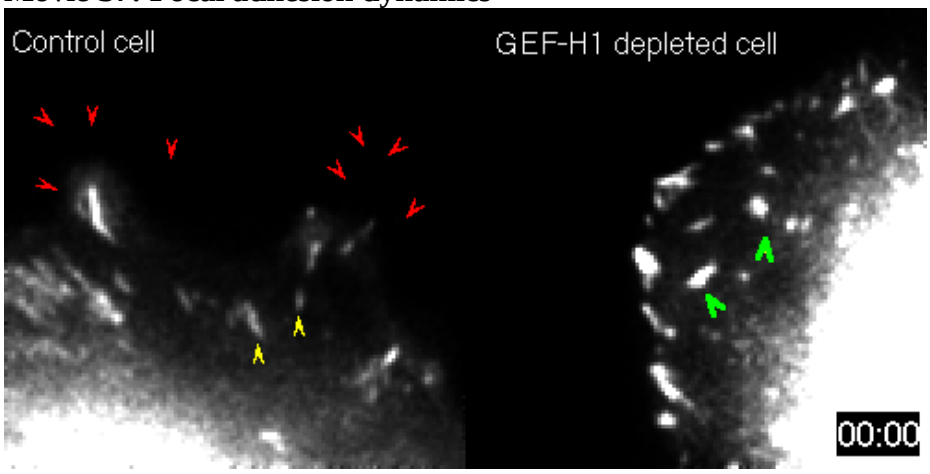

Movie S7: Focal adhesion dynamics in control and GEF-H1-depleted HeLa cells as depicted by EGFP-Paxillin time-lapse imaging. Red arrows indicate newly generated focal adhesions (FA). Yellow arrows in the control cell point to FA dissolving during the time-lapse series, whereas the green arrows point to FA in GEF-H1-depleted cells that do not turn over during the entire movie. Time-frame = 5 sec.

Movie S8: Small focal complex formation

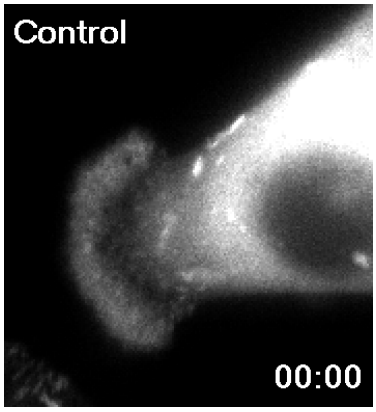

Movie S8: Movie showing EGFP-paxillin time-lapse imaging of control cell with strong ruffle activity. Comparably small EGFP-positive dots decorate the leading edge. Time-frame = 5 sec.

Movie S9A: Bright-field and EGFP-Paxillin time-lapse of control cell

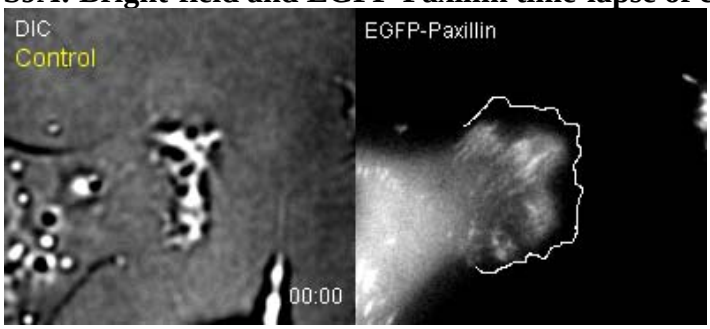

Movie S9B: Bright-field and EGFP-Paxillin time-lapse of GEF-H1 siRNA treated cell

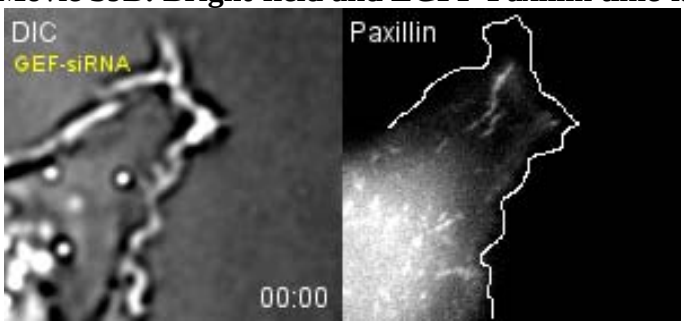

Movie S9A and Movie S9B: Extensions in GEF-H1 siRNA treated cells do not adhere properly. Live-cell imaging of Hela cells expressing EGFP-Paxillin. Cells were transfected with control or GEF-H1 targeting siRNA 48hrs prior to transfection with EGFP-Paxillin construct. After over-night protein expression, imaging was performed. Control cell movie S8A shows a typical control protrusion with extensions of modest size (see also Figure 3B, main manuscripts). Throughout the movie, small focal complexes are visible in close proximity of the dynamic edge (yellow arrows in the movie). In movie S9B, no new focal complexes are established after generation of the large extension in the cell treated with GEF-H1 siRNA leading to the collapse of the dynamic structure. Larger FA are visible at the stable (not dynamic) cell edge. Time-frame = 5 sec.

Movie S10: DIC movie of control Hela cells

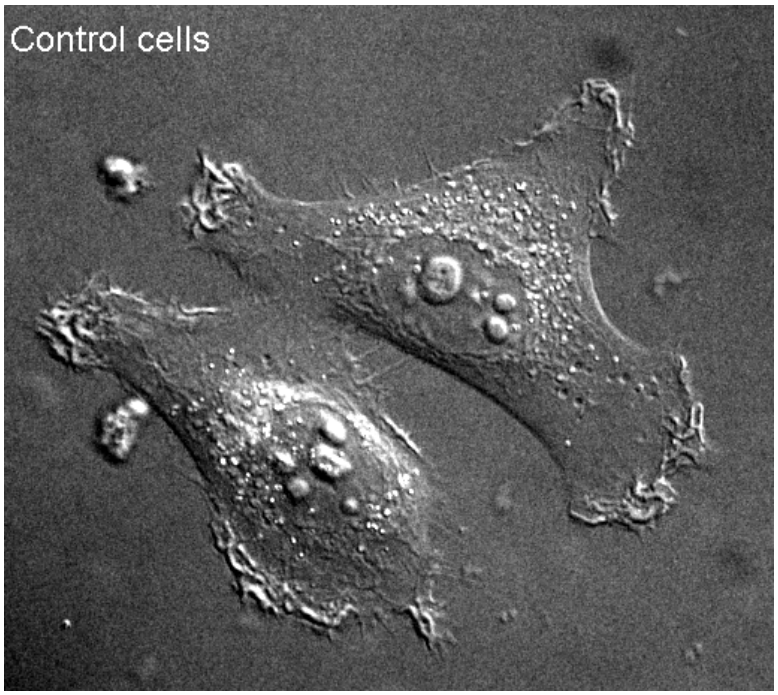

Movie S10: Ruffling dynamics in control cells. Corresponding movie to Figure S3. Frame-rate: 10 sec. Duration: 6 min.